Computation of Helicopter Rotor Acoustics in Forward Flight

Roger Strawn
Rupak Biswas

The Research Institute of Advanced Computer Science is operated by Universities Space Research Association, The American City Building, Suite 212, Columbia, MD 21044, (410) 730-2656

Work reported herein was supported by NASA via Contract NAS 2-13721 between NASA and the Universities Space Research Association (USRA). Work was performed at the Research Institute for Advanced Computer Science (RIACS), NASA Ames Research Center, Moffett Field, CA 94035-1000.

COMPUTATION OF HELICOPTER ROTOR ACOUSTICS IN FORWARD FLIGHT

Roger C. Strawn
US Army AFDD, ATCOM, MS 258-1

Rupak Biswas
RIACS, MS T27A-1

NASA Ames Research Center
Moffett Field, CA 94035-1000

Abstract

This paper presents a new method for computing acoustic signals from helicopter rotors in forward flight. The aerodynamic and acoustic solutions in the near field are computed with a finite-difference solver for the Euler equations. A nonrotating cylindrical Kirchhoff surface is then placed around the entire rotor system. This Kirchhoff surface moves subsonically with the rotor in forward flight. The finite-difference solution is interpolated onto this cylindrical surface at each time step and a Kirchhoff integration is used to carry the acoustic signal to the far field. Computed values for high-speed impulsive noise show excellent agreement with model-rotor and flight-test experimental data. Results from the new method offer high accuracy with reasonable computer resource requirements.

Introduction

In addition to the desire for high aerodynamic performance, modern helicopter designs also aim for low rotor noise. This is particularly important for civilian helicopters that operate near heavily populated areas.

There are two main types of noise that cause problems for helicopters. The first type is noise that is due to the interaction of the rotor blades with their vortical wake systems. This type of noise is called blade-vortex interaction, or BVI, noise. The second type of noise is called high-speed impulsive, or HSI, noise. It is characterized by a strong acoustic disturbance that occurs over a very short period of time. Impulsive noise is generally associated with high tip speeds and advancing tip Mach numbers greater that 0.9.

Accurate prediction of rotor noise is essential for its control. The most commonly used noise prediction techniques are based on the Ffowcs Williams and Hawkings equation [1]. This approach contains terms that model three different components of rotor noise. The first two components are thickness noise and loading noise. These are computed from the linear superposition of integrated monopole and dipole sources over the surface of the blade. The third term is a nonlinear quadrupole integral that is much more difficult to evaluate and typically neglected. Examples of this type of acoustics model are given in Refs. [2-3].

The difficulty in modeling the nonlinear quadrupole term is the main drawback with acoustics models that are based on the Ffowcs Williams and Hawkings equation. Without this term, the acoustic signals in the far field are typically underpredicted as shown in Ref. [4].

Improved accuracy has been obtained with alternate methods that are based on nonlinear computational fluid dynamics (CFD). For example, Baeder [4] solved the Euler equations to model the acoustics of rotor blades both in hover and in forward flight. Acoustic solutions were obtained at distances of up to 3.5 radii from the rotor hub. The problem with this approach is that the demand for computer resources increases exponentially as the solution domain is extended beyond the rotor blade. It is not currently practical to propagate helicopter acoustic waves much beyond 3 rotor radii without excessive numerical dissipation.

A third approach to rotor acoustic prediction uses the combination of a CFD method close to the rotor blade and a linear Kirchhoff integral formula to carry the acoustic solution to the far field. The Kirchhoff integral approach, such as that in Ref. [5], integrates a known pressure field over a prescribed surface and then propagates this signal to arbitrary distances from the rotor blade. The CFD method accurately captures the transonic flow nonlinearities close to the blade, while the Kirchhoff integral scheme is computationally more efficient over large distances.

Two types of hybrid CFD/Kirchhoff methods have been demonstrated for rotary-wing applications. The two methods differ as to whether or not the Kirchhoff surface rotates with the blade. Lyrintzis et al. [6-8] use a Kirchhoff surface that rotates with the blade. Pressure data on the

*Presented at the 19th Army Science Conference, 20-24 June, 1994, Orlando, Florida.

Kirchhoff surface are computed from a numerical solution of the full-potential equations. The Kirchhoff integral for the moving surface is computed with the formulation given in Ref. [5]. This approach has the advantage that the Kirchhoff integral uses the same computational mesh as the CFD calculation. Also, the Kirchhoff surface can be positioned to minimize numerical dissipation in the CFD solution.

However, this rotating-surface Kirchhoff formulation has one major problem. The Kirchhoff integral in Refs. [5-8] assumes that the Kirchhoff surface moves subsonically. Evaluation of the integral for a surface that moves supersonically is much more difficult and has not been successfully applied to a helicopter problem.

Restriction of the Kirchhoff integral to subsonic surface motion can be a major problem for high-speed rotary-wing applications. This is because the rotating velocity increases as Ωr, where Ω is the blade angular velocity and r is the distance in the plane of the rotor from the hub to a point on the Kirchhoff surface. For the high-speed test case computed later in this paper, a rotating Kirchhoff surface must be located less than 1.4 chords from the tip of the blade in order to ensure subsonic motion. This location may be too close for accurate acoustic predictions because the strong aerodynamic shock on the blade surface creates nonlinearities near the tip.

The acoustic prediction methods in Refs. [3,9] do not have this problem with supersonic motion of the Kirchhoff surface. This is because the integral evaluations take place on a nonrotating surface. A coordinate transformation is used to interpolate the near-field CFD solution onto a nonrotating, cylindrical Kirchhoff surface. The challenge with this method is whether the CFD solution can carry the acoustic signal out to the Kirchhoff cylinder with low numerical dissipation. However, there is no constraint on the radial location of the surface as long as it completely encloses the rotor blades.

Baeder et al. [3] have used a structured-grid Euler CFD solver and the nonrotating Kirchhoff formulation to compute HSI noise for a hovering rotor. Strawn et al. [9] have used a similar scheme, but their Euler solver used unstructured, solution-adaptive grids to improve the resolution of the near-field acoustic signals. Both methods have shown excellent agreement with experimental data for HSI noise from hovering rotors.

Both the Baeder et al. [3] and Strawn et al. [9] Kirchhoff integration schemes were limited to hovering rotors. Rotors in forward flight are significantly more difficult because the CFD solutions must be computed and stored at many time steps for the unsteady flowfield. The purpose of the current work is to develop a new CFD/Kirchhoff scheme for predicting helicopter acoustics in forward flight. The new formulation uses a nonrotating Kirchhoff surface that moves subsonically with the rotor hub. The Kirchhoff integral is evaluated with the formulation given in Ref. [5]. Development of appropriate data structures and efficient interpolation schemes are the primary tasks in this effort.

This is the first time that a nonrotating Kirchhoff surface has been used to compute the acoustics from rotors in forward flight. Results from the method are compared to experimental data for HSI noise. Solution accuracy is addressed and computed solutions exhibit minimal numerical dissipation. The overall computational efficiency of the method is also discussed.

Near-Field CFD Solution

The structured-grid Euler/Navier-Stokes solver called TURNS [10,11] is used to compute the aerodynamic field close to the helicopter rotor. This CFD code solves the Navier-Stokes equations about rotating helicopter blades. Since viscous effects are minimal for the test cases considered in this paper, the TURNS code is run in an inviscid mode.

The two computed cases in this paper were experimentally tested by Schmitz et al. [12]. They consist of a 1/7 scale research model of a US Army AH-1 helicopter with a blade aspect ratio of 9.22. Both cases have the same hover-tip Mach number of 0.665, with advance ratios of 0.258 and 0.348, respectively.

Identical computational grids for the TURNS code have been constructed for both test cases. They consist of a series of 50 C-meshes that are stacked in the spanwise direction, with 20 located on the blade surface. Because the computed cases are nonlifting, the problem is symmetric about the plane of the rotor. This means that the solution need only be computed over half the computational domain. Each C-mesh is located along a constant radial line from the hub of the rotor and contains 68 points in the chordwise direction with 48 points on the lower surface of each airfoil section. 35 points are located in the direction normal to the blade surface.

A view of the CFD mesh in the plane of the rotor is shown in Fig. 1. Note that the computational domain extends out to 2 rotor radii from the hub in the plane of the rotor. The outer boundary of the grid below the rotor blade is set at 1.5 radii. Between the blade tip and the outer spanwise

boundary, the clustered region of the mesh is swept backwards in an effort to capture the acoustic signal with minimal numerical dissipation.

Similar solutions for these cases were computed on similar grids by Baeder [4], who also used the TURNS code. In that study, however, the acoustic field was computed directly with the CFD code and the Kirchhoff surface approach was not used. Because of this, Baeder's CFD solutions covered a much larger computational domain in the spanwise direction than in the current work. In spite of these differences, the acoustic solutions near the blade tip in this paper are virtually identical to those computed by Baeder.

The TURNS code is first run in the quasi-steady mode to determine a starting solution at zero degrees azimuth angle. This requires approximately 1800 iterations corresponding to 24 CPU minutes on a Cray C-90 computer. The unsteady time marching is then started with each time step corresponding to 0.25 degrees of blade azimuth angle. Approximately one hour of C-90 CPU time is required to complete a full 360° of rotor motion.

The TURNS code has been modified so that the acoustic pressure, p, as well as its normal and temporal derivatives, p_n, and p_t, are computed at each time step. Note that the p_t derivative must be computed in a nonrotating reference frame so that it is compatible with the nonrotating Kirchhoff surface. Pressure values that are located on the Kirchhoff surface are written out to a file at intervals of one degree of azimuthal angle. This time-dependent data base is later used to evaluate the Kirchhoff integral.

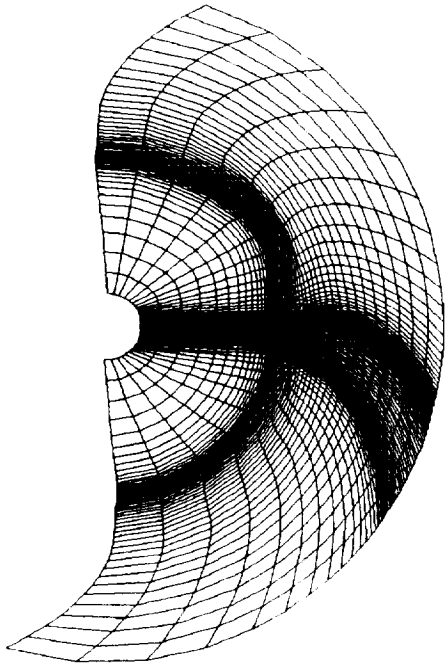

Figure 1: View of the 3-D CFD grid in the plane of the rotor.

Kirchhoff Surface Method

It is not practical to continue the CFD solution to large distances in the spanwise direction. Large numbers of mesh points are required and the calculation rapidly becomes too large for existing computers. An alternate approach is to place a nonrotating cylindrical Kirchhoff surface around the rotor blades as shown in Fig. 2. Strictly speaking, the Kirchhoff surface should completely enclose the rotor blades, but the top and bottom surfaces are neglected for these computations. They are located so far above and below the rotor plane that their contributions to the far-field acoustics are typically very small. Most of the rotor noise is produced in the plane of the rotor.

The Kirchhoff surface translates with the rotor hub when the helicopter is in forward flight. The acoustic pressure, p, at a fixed observer location, $\vec{x}$, and observer time, t, can be evaluated by performing the following integration on the cylindrical surface:

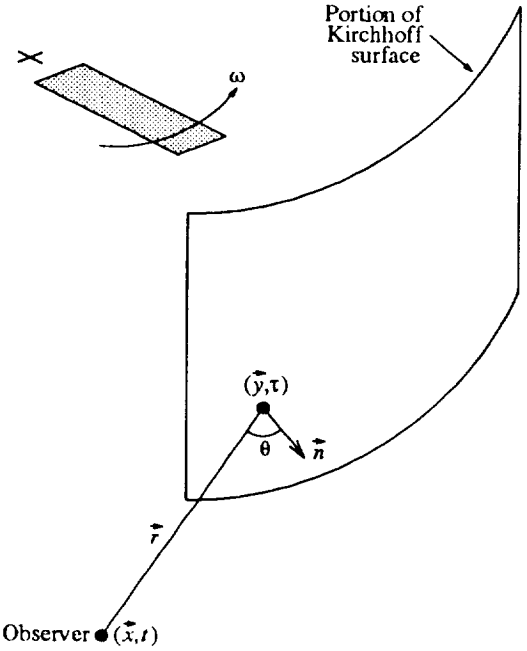

Figure 2: Schematic for the Kirchhoff surface integration.

$$p(\vec{x},t) = \frac{1}{4\pi}\int_S \left\{ \frac{E_1}{r(1-M_r)} + \frac{E_2 p}{r^2(1-M_r)} \right\}_\tau dS \quad (1)$$

This formulation is taken from Ref. [5]. It assumes that the Kirchhoff surface is moving with Mach number $\vec{M}$. The distance between a point on the Kirchhoff surface and the observer is given by $|\vec{r}|$, as shown in Fig. 2. Also note that the entire integral in Eq. (1) is evaluated at the time of emission for the acoustic signal, τ.

The expressions for E_1 and E_2 are given as:

$$E_1 = (M_n^2 - 1)p_n + M_n \vec{M}_t \cdot \nabla p - \left[\frac{M_n p_t}{a_\infty}\right] - \left[\frac{(\cos\theta - M_n)p_t}{a_\infty(1-M_r)}\right] \quad (2)$$

$$E_2 = \left[\frac{1-M^2}{(1-M_r)^2}\right](\cos\theta - M_n) \quad (3)$$

These expressions assume that the surface is moving with steady translational motion. Additional terms that are required to account for unsteady or rotational motion are given in Ref. [5]. The expression for E_2 in Eq. (3) has been modified from the original Farassat and Meyers' [5] formula by using the simplified expression found in Ref. [13].

In the above equations, M_n and M_r are the components of $\vec{M}$ along $\hat{n}$ and $\hat{r}$ in Fig. 2. $\vec{M}_t$ is the velocity vector tangent to the Kirchhoff surface, and ∇p is the gradient of the pressure on the Kirchhoff surface. The freestream speed of sound is assumed to be uniform at a_∞, and the angle, θ, is defined in Fig. 2.

Evaluation of the integral in Eq. (1) at the emission time requires a series of coordinate transformations to properly access the CFD database on the Kirchhoff surface. These transforms can be described with the aid of Fig. 3. Fig. 3a shows the rotor blade and Kirchhoff surface at the time the sound reaches the observer. However, Eq. (1) requires that the pressures on the Kirchhoff surface be evaluated at the time they were emitted. At the time of emission, both the Kirchhoff surface and the rotor blade were in different locations.

In order to find these locations, the delay between the observer time, t, and the emission time, τ, must first be computed. This can be determined from Fig. 3b by noting that the time it takes the acoustic signal to travel from the Kirchhoff surface to the observer is equal to the time it takes the translating Kirchhoff surface to move the distance, d. These

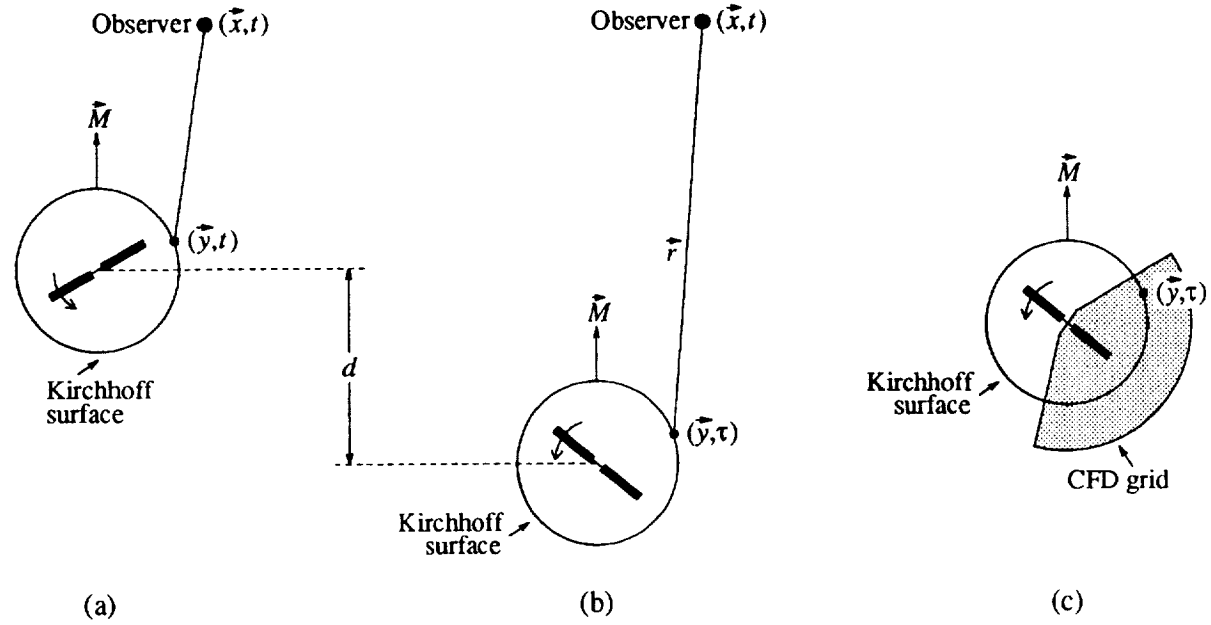

Figure 3: Two successive coordinate transformations are applied to evaluate the pressure data on the Kirchhoff surface.

times are given as $|\vec{r}|/a_\infty$, and $da_\infty/|\vec{M}|$, respectively. This leads to a quadratic equation for the required time delay. One of the roots is nonphysical and can be discarded. The locations of the Kirchhoff surface and the rotor blade at the emission time can then be computed.

Once the geometry is established at the emission time, the acoustic pressures and their derivatives on the Kirchhoff surface are interpolated from the stored CFD database (see Fig. 3c). The CFD solutions are stored at discrete time steps on the Kirchhoff surface as two-dimensional quadrilateral meshes. The required acoustic data are determined by linear interpolation in time and space.

This procedure must be performed for every discrete integration point on the Kirchhoff surface. Typical grid sizes for this integral evaluation are 1440 points in the azimuthal direction and 100 points normal to the plane of the rotor. The azimuthal points are equally spaced to enclose both rotor blades. The vertical extent of the Kirchhoff surface is ±1.5 rotor radii, the same as that for the CFD grid. The point spacings in this direction are exponentially stretched from the plane of the rotor to the outer boundaries.

Results

The new hybrid CFD/Kirchhoff method has been used to predict the acoustic signals from two model-rotor wind-tunnel cases described in Ref. [12]. These experiments recorded acoustic signals from a 1/7 scale model of the Army's AH-1 helicopter main rotor. Microphones were placed at several fixed locations around the rotor system. Scaled acoustic data from flight tests is also reported in Ref. [12].

The two computed test cases both a have hover-tip Mach number, M_{tip}, equal to 0.665. The advance ratios, μ, for the low-speed and high-speed cases are 0.258 and 0.348, respectively. The rotor thrust coefficient is the same for both cases and is equal to 0.0054. These rotor blades have symmetric airfoil sections with a thickness-to-chord ratio of 0.0971 and an aspect ratio of 9.22. The primary noise-generation mechanism in both cases is high-speed impulsive (HSI) noise.

In spite of the fact that the model rotor experiments have a significant amount of thrust, the computations in this paper are for nonlifting rotors with the collective pitch set to zero. This simplifies the analysis since the rotor wake does not have to be modeled in the CFD solution. In general, this is a complicated task and is not the focus of this paper.

The justification for neglecting the rotor thrust is that HSI pressure signals in the plane of the rotor are generally insensitive to thrust. This has been experimentally documented by Schmitz et al. [12,14]. The nonlifting assumption in the analysis has little effect on the computed results as long as acoustic comparisons are restricted to the plane of the rotor. Acoustic predictions that are out of the rotor tip path plane will require realistic rotor wake models in the CFD solutions. This is particularly true for cases with blade-vortex interactions.

The Kirchhoff surface is located at 1.39 rotor radii for both computations. This location is far enough from the blade tip that nonlinear transonic effects are small, but close enough so that numerical dissipation does not degrade the CFD solution. Both Baeder et al. [3] and Strawn et al. [9] have investigated the choice of Kirchhoff surface locations for high-speed hovering rotors. Their results show grid independence for Kirchhoff surfaces at 1.4 radii.

If comparisons to experiment are restricted to the plane of the rotor, then the Kirchhoff integration is symmetric about this plane. This means that the integral in Eq. (1) need only be computed over half of the Kirchhoff surface. The resulting pressure can then be doubled to account for the remainder of the integration. As such, the numerical integration on the Kirchhoff surface consists of 1440 equally-spaced points around the azimuth and 50 unequally-spaced points in the lower half-plane of the rotor blade.

With this grid, the Kirchhoff integration in Eq. (1) requires about 30 CPU seconds on the Cray C-90 for each evaluation of the observer pressure. Most of this time is spent performing interpolations in the CFD database. There is a potential for significant speedup if these interpolations can be performed more efficiently.

Typical acoustic pressure signals in this paper consist of approximately 24 evaluations of the observer pressure. This requires a total CPU time of 12 minutes to obtain the complete acoustic signal at each observer location. At large distances from the rotor blade, this is orders of magnitude less than the time that would be required to compute a pure CFD solution for the same location.

Figure 4 compares the computed and experimental results for the low-speed case. This case has an advancing-tip Mach number, M_{at}, of 0.837 and the computations show significant transonic flow at the blade tip. This transonic flow is limited to the blade and does not connect to the far-field region of supersonic flow relative to the blade. The

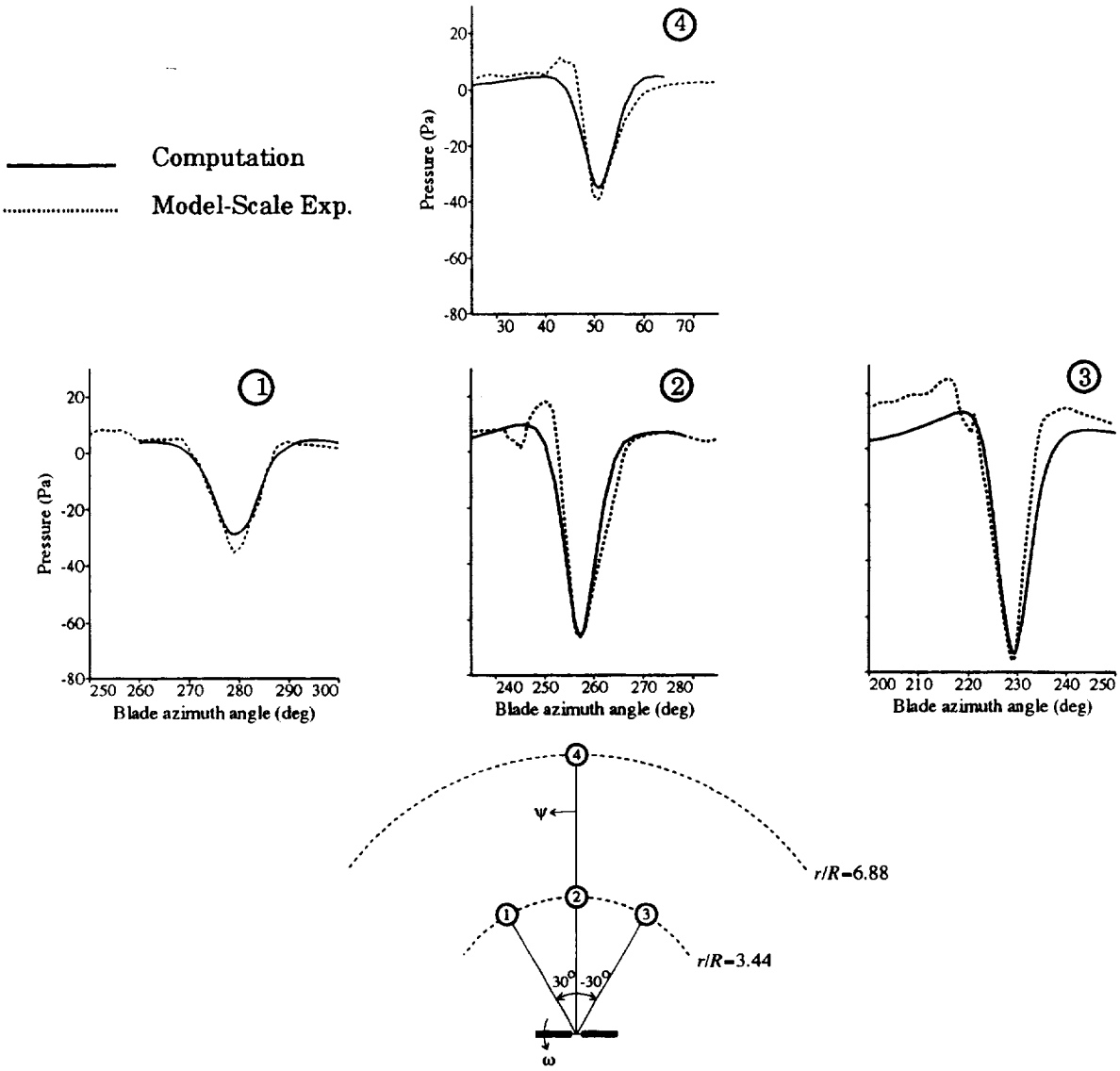

Figure 4: Acoustic pressure comparisons for M_{at} = 0.837.

experimental pressures in Fig.4 were obtained by manually digitizing the published data in Ref. [12]. As a result, the acoustic signal plots may deviate slightly from the original experimental data. Because this case is a windtunnel experiment, the observer location is fixed with respect to the rotor hub. The equivalent numerical simulation requires that the observer moves with the rotor hub in forward flight.

Excellent agreement is seen between experiment and computation for all of the microphone locations in Fig. 4. The first three microphones are located at 3.44 rotor radii while a fourth is located at 6.88 radii. The computed peak negative pressures and wave shapes are very close to their experimental counterparts. The directivity of the acoustic signal is also computed accurately. The loudest noise radiates toward the advancing side of the rotor disk (microphone 3).

Results for the high-speed case are shown in Fig. 5. The advancing-tip Mach number has been increased to 0.896, and the amplitudes of the acoustic disturbances are much higher than those in Fig. 4. The computed results show reasonably good agreement with the experimental data but the peak negative pressures are underpredicted uniformly by about 20 percent. Note that the maximum acoustic amplitude is now directed straight ahead (microphone 2). This is seen in both the experimental and computed results.

A possible reason for this underprediction of peak negative pressures is shown in Fig. 6. This figure shows computed Mach contours relative to the rotor blade in the tip path plane. The blade is located on the advancing side at 105° azimuth

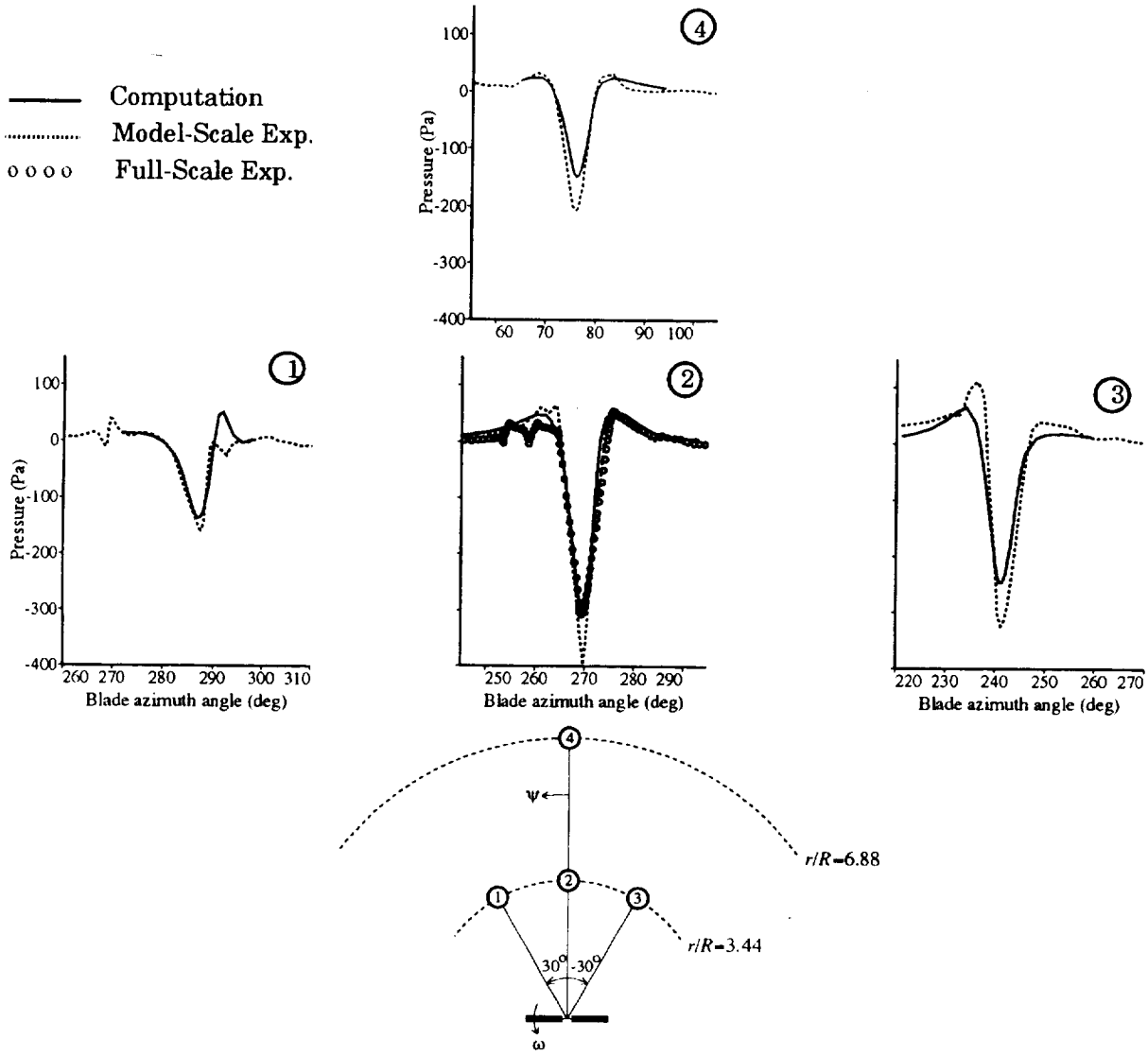

Figure 5: Acoustic pressure comparisons for M_{at} = 0.896.

angle, where the surface shock at the blade tip is the strongest. The Mach-one lines are drawn darker than the other contours. Note that the supersonic region on the blade surface almost connects with the supersonic region in the far field. When this phenomenon occurs, it is referred to as delocalization and the surface shock is free to propagate to the far field with very little dissipation. The acoustic amplitude increases dramatically at the onset of delocalization.

The delocalization phenomena is highly dependent on nonlinear transonic effects that occur near the blade tip. Fig. 6 shows that the flowfield is not quite delocalized, but it should be noted that this CFD solution was computed for a nonlifting rotor. If the cyclic pitch and wake effects were included in the computation, it is reasonable to assume that these might have some effect on the picture in Fig. 6. If these effects caused the flowfield to delocalize, then the predicted peak negative pressures would be larger, and thereby show better agreement with the experimental results.

Experimental data from the flight test are also shown for microphone 2 in Fig. 5. This flight-test data shows excellent agreement with the computer predictions but not with the model-scale results. The reasons for the discrepancies between model-scale and flight test are not known. Perhaps it is related to the sensitivity of the far-field acoustic pressures when the flowfield at the rotor tip is very close to delocalization.

In spite of these differences, the computed results in Fig. 5 are significantly better than those shown by other researchers. Baeder [4] computed this case with a pure CFD approach and obtained a peak negative pressure of 270 Pa for microphone

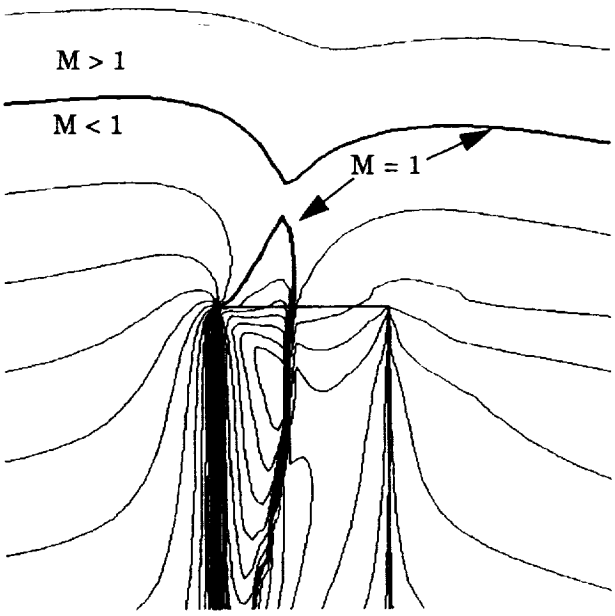

Figure 6: Mach contours at 105° for M_{at} = 0.896.

location 2. It is likely that part of this underprediction is caused by numerical dissipation in the numerical solution at 3.44 radii. The CFD mesh did not include the 6.88 radii location in that study. Baeder also mentions that linear methods based on the Ffowcs Williams and Hawkings equation predict a peak negative pressure of only 210 Pa for the same location. The current computation gives a peak negative pressure of 312 Pa compared to the experimental result of 397 Pa.

Discussion

The accuracy of the calculations can be addressed by examining both the fundamental approximations in the Kirchhoff formulation and the mesh independence of the computed results. The first assumption in the Kirchhoff formulation is that the Kirchhoff surface moves through undisturbed air. This is not entirely true for a helicopter because lifting rotor blades generate aerodynamic disturbances in their wake systems. The interaction of the acoustic signals with the rotor wake outside the Kirchhoff surface is not considered in the present method.. The effect of this approximation should be small however. This is because a rotor in forward flight propagates most of its acoustic disturbances ahead of it while the wake system is left behind. Thus there is little interaction between the forward-radiating acoustic signals and the rotor wake.

Another basic assumption is that the speed of sound is constant outside the Kirchhoff surface. This means that the surface must be located far enough from the rotor blade to completely enclose all nonlinear transonic effects. We can check whether this condition has been met for the computed results shown in Figs. 4 and 5 by performing a new computation with a different Kirchhoff surface location. If the predicted acoustic pressures differ, then there may be some nonlinear effects that are not completely inside the surface.

Figure 7 shows computed pressure signals for the high-speed test case at microphone location 2. The results differ in the positions of the Kirchhoff surfaces, s/R. The first prediction has a surface located at 1.39 radii and the second at 1.28. The two computed results are virtually identical, which indicates that the nonlinear effects are completely contained inside the Kirchhoff surface.

Figure 7 also provides evidence of grid independence of the CFD solution. If numerical dissipation played a role in the CFD solution, then the far-field acoustic pressures would be affected by the location of the Kirchhoff surface.

A final question involves the numerical resolution of the Kirchhoff integral in Eq. (1). The calculations in Figs. 4 and 5 used a 1440 x 50 mesh on the lower half of the Kirchhoff surface. This corresponds to a constant azimuthal resolution of 0.25°, and a minimum vertical resolution of 0.01 chords at the plane of the rotor. Figure 8 compares the original results for the high-speed case at microphone location 2 with those from a finer Kirchhoff

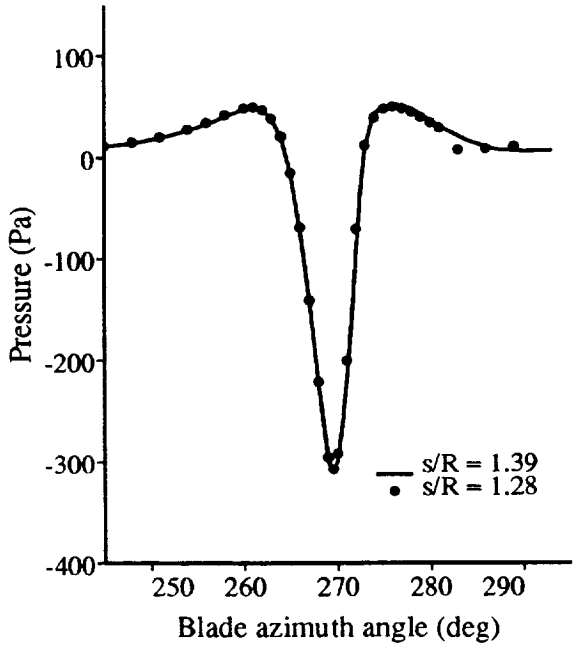

Figure 7: Comparison of results for microphone location 2 using two different Kirchhoff surfaces.

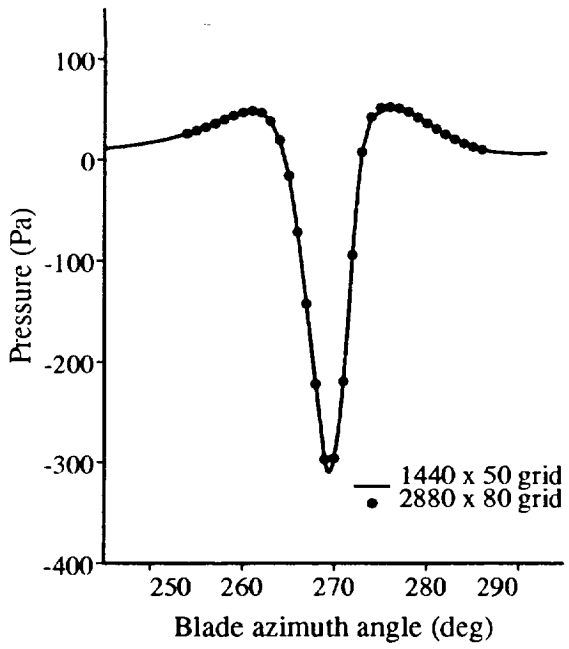

Figure 8: Comparison of results with two different mesh resolutions on the Kirchhoff surface.

mesh. This finer mesh has a resolution of 2880 x 80, where the minimum vertical spacing at the plane of the rotor has been decreased to 0.005 chords. The two results are virtually identical, indicating that the computed values from the original Kirchhoff integration are mesh independent.

Summary

This paper presents a new method for computing far-field acoustics from helicopter rotor blades in forward flight. A solution to the Euler equations accurately models the nonlinear effects near the blade surface and a Kirchhoff integration propagates the near-field acoustic signals to the far field in a computationally-efficient manner. The key to the Kirchhoff formulation is the use of a nonrotating surface which ensures that its motion is always subsonic.

Close to the blade tip, computed results with the new method compare favorably with experimental results and predictions from pure CFD methods. However, the major advantage of the new method over its pure CFD counterparts occurs for far-field calculations. CFD computations are generally limited to computational domains of less than 3 or 4 rotor radii. The combined CFD/Kirchhoff method can compute acoustic signals at arbitrary observer locations with minimal numerical dissipation.

Although the method is demonstrated for cases with high-speed impulsive noise, it should also be applicable to cases with blade-vortex interactions. The primary challenge for such computations will be the accurate modeling of the rotor wake system in the CFD solver.

References

[1] Ffowcs Williams, J. E., and Hawkings, D. L., "Sound Generated by Turbulence and Surfaces in Arbitrary Motion," Philosophical Transactions of the Royal Society, Vol. A264, May 1969, pp. 321-342.

[2] Brentner, K. S., "Prediction of Helicopter Rotor Discrete Frequency Noise - A Computer Program Incorporating Realistic Blade Motion and Advanced Acoustic Formulation," NASA TM-87721, Oct. 1986.

[3] Baeder, J. D., Gallman, J. M., and Yu, Y. H., "A Computational Study of the Aeroacoustics of Rotors in Hover," presented at the AHS 49th Annual Forum, St. Louis, MO, May 1993.

[4] Baeder, J. D., "Euler Solutions to Nonlinear Acoustics of Nonlifting Rotor Blades," presented at the International Technical Specialists Meeting on Rotorcraft and Rotor Fluid Dynamics, Philadelphia, PA, Oct. 1991.

[5] Farassat, F., and Myers, M. K., "Extension of Kirchhoff's Formula to Radiation from Moving Surfaces," Journal of Sound and Vibration, Vol. 123, No. 3, 1988, pp. 451-460.

[6] Lyrintzis, A. S., "The Use of Kirchhoff Method in Aeroacoustics," in Computational Aero and Hydro-Acoustics, FED Vol. 147, 1993, pp. 53-61.

[7] Xue, Y., and Lyrintzis, A. S., "The Use of a Rotating Kirchhoff Formulation for 3-D Transonic BVI Noise," presented at the AHS 49th Annual Forum, St. Louis, MO, May 1993.

[8] Lyrintzis, A. S., Xue, Y., and Kilaras, M. S., "The Use of a Rotating Kirchhoff Formulation for High-Speed Impulsive Noise," AIAA paper 94-0463, Jan. 1994.

[9] Strawn, R. C., Garceau, M., and Biswas, R., "Unstructured Adaptive Mesh Computations of Rotorcraft High-Speed Impulsive Noise," AIAA paper 93-4359, Oct. 1993.

[10] Srinivasan, G. R., Baeder, J. D., Obayashi, S., and McCroskey, W. J., "Flowfield of a Lifting Rotor in Hover: A Navier-Stokes Simulation," AIAA Journal, Vol. 30, No. 10, Oct. 1992, pp. 2371-2378.

[11] Srinivasan, G. R., and Baeder, J. D., "Turns: A Free-Wake Euler/Navier-Stokes Numerical Method for Helicopter Rotors," AIAA Journal, Vol. 31, No. 5, May 1993, pp. 959-962.

[12] Schmitz, F. H., Boxwell, D. A., Splettstoesser, W. R., and Schultz, K. J., "Model-Rotor High-Speed Impulsive Noise: Full-Scale Comparisons and Parametric Variations," Vertica, Vol. 8, No. 4, 1984, pp. 395-422.

[13] Meyers, M. K., and Hausmann, J. S., "Computation of Acoustic Scattering from a Moving Rigid Surface," Journal of Acoustical Society of America, Vol. 91, No. 5, 1992, pp. 2594-2605.

[14] Schmitz, F. H., Boxwell, D. A., and Vause, C. R., "High-Speed Helicopter Impulsive Noise," Journal of the American Helicopter Society, Oct. 1977, pp. 28-36.